Fast crystallization of chalcogenide glass for rewritable memories

Zhimei Sun' , Jian Zhou, Andreas Blomqvist, Börje Johansson, and Rajeev Ahuja

Citation: Appl. Phys. Lett. **93**, 061913 (2008); doi: 10.1063/1.2967742
View online: http://dx.doi.org/10.1063/1.2967742
View Table of Contents: http://aip.scitation.org/toc/apl/93/6
Published by the American Institute of Physics

Fast crystallization of chalcogenide glass for rewritable memories

Zhimei Sun,[1,a)] Jian Zhou,[1] Andreas Blomqvist,[2] Börje Johansson,[2] and Rajeev Ahuja[2]
[1]*Department of Materials Science and Engineering, Xiamen University, No. 422 Siming South Road, 361005 Xiamen, People's Republic of China*
[2]*Condensed Matter Theory Group, Department of Physics and Materials Science, Uppsala University, P.O. Box 530, SE-751 21 Uppsala, Sweden*

(Received 2 July 2008; accepted 16 July 2008; published online 15 August 2008)

By *ab initio* molecular dynamics simulations, we unraveled the unique network structure of amorphous $Ge_1Sb_2Te_4$, which shows high rank of ordering and mostly consists of distorted defective octahedrons with a small portion of distorted tetrahedrons. The phase transition from amorphous to cubic $Ge_1Sb_2Te_4$ would be mainly a process of angle rearrangements of tetrahedrons to octahedrons and vice versa. © *2008 American Institute of Physics*. [DOI: 10.1063/1.2967742]

In contrast to conventional good glass formers that are characterized by long crystallization time, chalcogenide (GST), a family of good glass formers, exhibits an extremely short crystallization time (in nanoseconds). Moreover, it can be switched rapidly back and forth between amorphous and crystalline states for millions of cycles, which makes rewritable data storage applications possible. Recently it is considered as one of the most promising candidate materials for nonvolatile electronic memories.[1–5] Both optical and electrical data storage rely on the extremely fast and reversible phase transition between the crystalline (rocksalt structure) and amorphous states of GST. The pronounced optical or electrical contrast indicates that the local atomic arrangement of the amorphous state differs considerably from that of its crystalline state. However, the fact that the atomic rearrangement required for the recrystallization of amorphous GST proceeds within a few nanoseconds[6] indicates that these two states should have similar local atomic arrangements. Therefore, a full understanding of the local atomic arrangements of GST is necessary to reveal the reversible phase change mechanism behind the utilization and thus to identify new phase-change materials with better performance. However, the mechanism has not been fully understood as yet although many efforts have been made.[5,7–12] Here by *ab initio* molecular dynamics (AIMD) simulations, we investigated the local atomic arrangements of amorphous $Ge_1Sb_2Te_4$ (*a*-GST124) to shed light on the fast reversible phase change between amorphous and crystalline states of GST alloys.

The AIMD methods used in the present work are implemented in the Vienna *ab initio* simulation package.[13] The interatomic forces were computed quantum mechanically using projector augmented wave methods[14] within the local density approximation. One *k* point (gamma) was used for the electronic structure calculations. Gaussian smearing was applied, and an energy cutoff of 136.4 eV was chosen. The initial configuration is a cubic GST124 supercell that contains 27 Ge, 54 Sb, and 108 Te atoms plus 27 vacancies, where Ge, Sb, and vacancies occupy one sublattice and Te atoms occupy the other sublattice of the rocksalt structure. A density of 0.0305 atoms/Å^3, which is close to the experimental value of the amorphous phase,[15] is used in the simulations. The supercell was first melted and thermalized at 3000 K for 3 ps, wherein the temperature was controlled using the algorithm of Nosé,[16,17] then it was gradually quenched down to 300 K at a quenching rate of 6.67×10^{13} K s^{-1}, and finally rethermalized at 300 K for 6 ps. The results presented in this paper are averaged over the configurations gathered during the final 3 ps period at 300 K.

Figure 1 shows the reduced partial pair correlation functions for *a*-GST124. Around Ge, the Ge–Te pair function predominates and shows a very sharp first peak at ~2.749 Å, which is quite shorter than the first nearest neighbor distance (3.03 Å) of cubic (*c*)-GST124, and a small second peak at ~6.088 Å, which is comparable to the third nearest neighbor distances (6.093 Å) of *c*-GST124. On the other hand, Ge–Ge and Ge–Sb pair functions are least important and develop into first, second, and third peaks. This indicates a medium range order around Ge. Around Te, Te–Ge and Te–Sb pair functions dominate and the Te–Te pair is least important. In contrast to the Te–Ge pair, the Te–Sb pair function shows a second peak at ~4.26 Å and a third peak at ~6.22 Å that are comparable to the distances of the second (~4.30 Å) and third (6.093 Å) nearest neighbors in *c*-GST124, respectively.

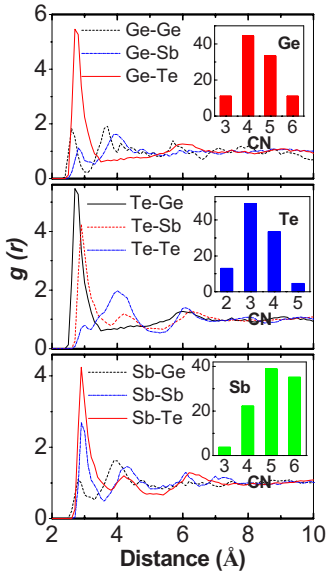

FIG. 1. (Color online) The calculated partial pair correlation function $g(r)$, wherein the insets show the fractional distribution of coordination number around Ge, Te, and Sb.

a)Author to whom correspondence should be addressed. Electronic addresses: zmsun@xmu.edu.cn and zhmsun2@yahoo.com.

TABLE I. The estimated coordination number (Z) for various pairs of atoms in a-GST124,. where the cutoff radius is the first minimum of the corresponding $g(r)$.

	With Ge	With Sb	With Te	Z_{total}
Ge	0.21	0.32	4.11	4.64
Sb	0.16	1.07	3.74	4.97
Te	1.03	1.87	0.36	3.26

The Te–Te pair function is rather interesting by showing a very broad first peak at ~4.13 Å with a tiny shoulder at a lower distance and a second peak at ~6.09 Å, which are comparable to the second and third neighbor distances of the Te–Te bond in c-GST124, respectively. This shows a high ordering around Te atoms in a-GST124, which resembles that of its cubic state because there is no Te–Te bond existing as the first nearest neighbor in c-GST124. The same rule is applicable to Sb atoms, which also show a medium range order, as seen from the structures at the second and third peaks.

The partial and total coordination numbers (Z) for each element can be estimated by integrating the partial pair correlation functions. As listed in Table I, the major contribution to Ge are the Ge–Te bonds with a small proportion of Ge–Ge and Ge–Sb bonds. The total coordination number of 4.64 suggests a mixture of multifold coordinated Ge in a-GST124 in contrast to the tetrahedrally bonded Ge, as proposed in the above models.[5,12] The same rule can be applied to Sb and Te. As an average, the total coordination numbers of 4.64, 4.97, and 3.26 for Ge, Sb, and Te are significantly lower than the ideal octahedral coordination of 6, 6, and 4.5, respectively. The rather defective coordination in a-GST124 may account for the pronounced differences in optical and electrical properties between its amorphous and cubic states. Furthermore, as seen in the inset in Fig. 1, which shows the fraction distribution of the coordinations number for various species, fourfold and fivefold coordinations dominate Ge, threefold and fourfold coordinations predominate Te, and fivefold and sixfold coordinations dominate Sb. This clearly shows a picture of the multifold coordinated system.

Further insight on a-GST124 is gained by analyzing the (first-neighbor) bond angle distributions, which is shown in Fig. 2. Sharp peaks centered at ~88°, ~92°, and ~88° are observed around Ge, Sb, and Te, respectively, which reminisces the octahedral geometry of rocksalt structured GST124, while the presence of a small broad peak at ~165°

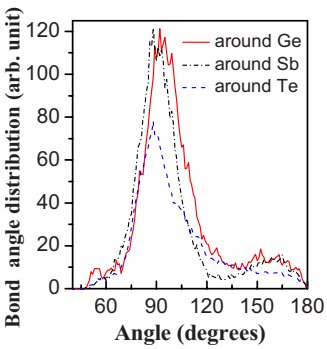

FIG. 2. (Color online) Bond angle distributions calculated around Ge (solid), Sb (dash), and Te (solid dot) in a-GST124, where the cutoff distance to the calculated bond angle is 3.5 Å.

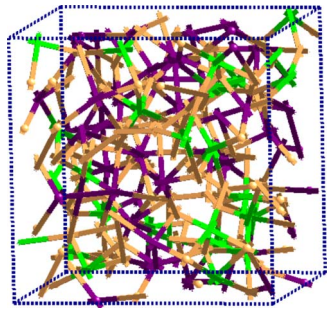

FIG. 3. (Color online) A snapshot structure of a-GST124, where the light grey atoms represent Te, the black atoms represent Sb, and the dark grey atoms represent Ge.

indicates a distorted octahedrally coordinated a-GST124. As seen from a snapshot of a-GST124 in Fig. 3, angles at ~90° dominate the bonding network of the multifold coordinated atoms. Furthermore, both odd- and even-number rings are also observed in a-GST124 in contrast to the model of an even-number ring amorphous structure.[8] A close investigation of the local atomic arrangements of a-GST124 shows that roughly around 37% Ge, 11% Sb, and 15% Te are in a tetrahedral environment, while the remaining atoms occupy defective octahedral sites. The tetrahedral geometry is visible from small shoulders at ~109°, ~108°, and ~106° around Ge, Sb, and Te atoms in the angle distributions in Fig. 2, respectively. A further study of the structure of a-GST124 shows highly distorted tetrahedrons since the bond angles are not exactly 109° but have a broad range from ~65° to ~135°, with the average value being ~109°. In addition, most octahedrons are also distorted with a bond angle distribution range from ~65° to ~100°. Compared to the octahedral symmetry of c-GST124, this could render the phase transition from amorphous to crystalline state easier as it would involve the angle rearrangements of tetrahedrons into octahedrons.

Figure 4 shows some typical angle distributions for various pairs of bonds in a-GST124 with respect to the [100] or [010] direction of c-GST124. It is obvious that there is a correlation in the Ge–Ge, Sb–Sb, Ge–Sb, and Te–Te bonds as demonstrated by the sharp peaks at ~45°, ~60°, ~90°,

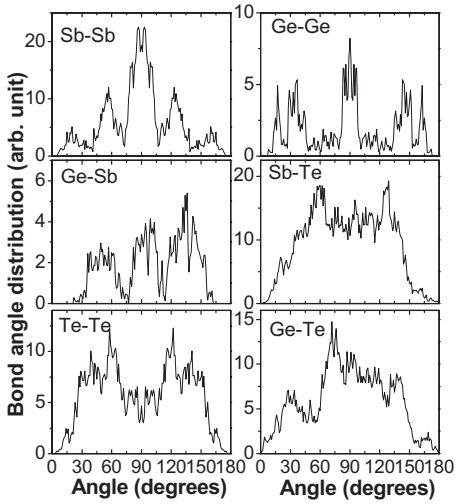

FIG. 4. Distribution of angles for various bond pairs (Ge–Ge, Ge–Sb Sb–Te, Te–Te, and Ge–Te) with respect to the [100] direction and that of Sb–Sb with respect to the [010] direction.

~120°, ~135°, etc. The Ge–Te and Sb–Te bonds seem more or less uncorrelated as seen from the broad distributed angles. Compared to the corresponding angles of ~45°, ~90°, and ~135° for *c*-GST124, it clearly indicates a highly local ordering in *a*-GST124.

In summary, through the AIMD study we have shown that the total coordination numbers for Ge, Sb, and Te atoms in *a*-GST124 are much lower than those of its rocksalt structure, while the bond angles of the nearest neighbors are close to its cubic state. We have also shown that most species occupy distorted defectively octahedral sites, while the remaining atoms are in a distorted tetrahedral environment. As a result, the phase transition from an amorphous to a cubic state would be a process of angle rearrangements of the small portion of distorted tetrahedrons to octahedrons and vice versa. It is this unique character that results in the fast and reversible phase transition between amorphous and rocksalt states hundreds of thousand times without fatigue. Furthermore, the present results may also give a clue for studying the formation mechanism of bulk metallic glasses, which is still an open question so far.

Z. M. S. acknowledges support from the Natural Science Foundation of Fujian Province of China (No. 2008J0166) and Xiamen University (No. X071I4). Computational resources provided by UPPMAX high-performance clusters of Uppsala University are also acknowledged.

[1] M. H. R. Lankhorst, B. W. S. M. M. Ketelaars, and R. A. M. Wolters, Nat. Mater. **4**, 347 (2005).
[2] H. F. Hamann, M. O'Boyle, Y. C. Martin, M. Rooks, and H. K. Wickramasinghe, Nat. Mater. **5**, 383 (2006).
[3] M. Wuttig and N. Yamada, Nat. Mater. **6**, 824 (2007).
[4] S. Tyson, G. Wicker, S. Hudgens, and K. Hunt, *Aerospace Conference Proceedings, 2000 IEEE* 5, 385–390 (2000).
[5] A. V. Kolobov, P. Fons, A. I. Frenkel, A. L. Ankudinov, J. Tominaga, and T. Uruga, Nat. Mater. **3**, 703 (2004).
[6] M. Chen, K. A. Rubin, and R. W. Barton, Appl. Phys. Lett. **49**, 502 (1986).
[7] D. A. Baker, M. A. Paesler, G. Lucovsky, S. C. Agarwal, and P. C. Taylor, Phys. Rev. Lett. **96**, 255501 (2006).
[8] S. Kohara, K. Kato, S. Kimura, H. Tanaka, T. Usuki, and K. Suzuya, Appl. Phys. Lett. **89**, 201910 (2006).
[9] Z. M. Sun, J. Zhou, and R. Ahuja, Phys. Rev. Lett. **96**, 055507 (2006).
[10] Z. M. Sun, J. Zhou, and R. Ahuja, Phys. Rev. Lett. **98**, 055505 (2007).
[11] W. Wełnic, A. Pamungkas, R. Detemple, C. Steimer, S. Blügel, and M. Wuttig, Nat. Mater. **5**, 56 (2006).
[12] C. Bichara, M. Johnson, and J. P. Gaspard, Phys. Rev. B **75**, 060201(R) (2007).
[13] G. Kresse and J. Hafner, Phys. Rev. B **47**, 558 (1993).
[14] G. Kresse and D. Joubert, Phys. Rev. B **59**, 1758 (1999).
[15] W. K. Njoroge, H. W. Wöltgens, and M. Wuttig, J. Vac. Sci. Technol. A **20**, 230 (2002).
[16] S. Nosé, Prog. Theor. Phys. Suppl. **103**, 1 (1991).
[17] D. M. Bylander and L. Kleinman, Phys. Rev. B **46**, 13756 (1992).